Amplification of broadband noise pumped by two lasers in optical fibers

J. M. Chávez Boggio, S. Tenenbaum, and H. L. Fragnito

Optics and Photonics Research Center, Instituto de Física "Gleb Wataghin," Unicamp, Campinas 13083-970, SP, Brazil

Received September 28, 2000; revised manuscript received March 23, 2001

A theoretical and experimental investigation of catastrophic amplification of broadband noise in optical fibers near the zero-dispersion frequency (ν_0) pumped by two lasers with frequencies that are symmetrically tuned relative to ν_0 is presented. The effect is due to a four-wave mixing (FWM) process, phase matched up to third-order dispersion, between the spectral components of noise and the lasers. We observed a FWM gain of 16 dB (10-dB net gain) over a 22-nm bandwidth (limited by fourth-order dispersion) for 18-dBm power lasers at ± 1 THz (8 nm) from ν_0 in a 25-km-long dispersion-shifted fiber. A simple analytical model is proposed that will permit us to investigate this effect numerically in amplified links with concatenated amplifiers and consider random fluctuations of ν_0 along the fiber.

OCIS codes: 060.4370, 060.4510, 060.2330.

1. INTRODUCTION

Four-wave mixing (FWM) between channels in dense wavelength-division multiplexing (DWDM) systems is known to severely limit the transmission capacity of optical fibers.[1] These FWM interactions are particularly detrimental if one of the channels operates at the zero-dispersion wavelength, λ_0 (Ref. 2) (or, more rigorously speaking, slightly above λ_0 in the anomalous dispersion region[3]). In this case, the FWM is nearly phase matched, leading to efficient buildup of FWM products.[2] Phase-matched FWM can also occur between a single channel at λ_0 and Fourier components in the amplified spontaneous emission (ASE) noise from optical amplifiers, leading to efficient amplification of noise in the fiber.[4–10] Following Marcuse,[4] we refer to this efficient mechanism for energy transfer from lasers into noise as catastrophic noise buildup.

In this paper we show that catastrophic noise buildup can also occur in the presence of two lasers, even if neither one is tuned to λ_0. Experimentally, we observed broadband noise amplification with gain in excess of 15 dB when lasers were tuned nearly symmetrically relative to the zero-dispersion frequency of the fiber. This effect is due to a FWM process between two lasers and noise. The analysis of this process differs from that describing two-pump parametric amplification of a weak laser signal[11,12] in that the noise field is broadband and stochastic, in contrast with the laser signal field, which is narrow band and coherent.

In general, with two input lasers (frequencies ν_1 and ν_2) several FWM processes are possible that involves these lasers and a noise Fourier component at ν. These interactions produce overtones at $\nu_1 + \nu_2 - \nu$, $\nu_1 - \nu_2 + \nu$, $2\nu_1 - \nu$, etc. In addition, FWM among the lasers (producing tones at $2\nu_1 - \nu_2$ and $2\nu_2 - \nu_1$) and a cascaded FWM process along the fiber exhibit a complicated cacophony as all Fourier components become coupled to one another. A nonlinear Schrödinger equation (NLSE) fully accounts for all laser–laser and laser–noise interactions. In fact, we have found good agreement between our experimental results and numerical solution of the NLSE. However, this approach does not provide physical insight into the ways in which the individual FWM processes are responsible for the features in the output spectrum. In Section 2 we present a different approach in which we isolate a given FWM process and neglect the others. The experimental observations are well described by the $\nu_1 + \nu_2 - \nu$ process, for which we present a detailed analysis. We show that, when the lasers are tuned nearly symmetrically relative to ν_0, only this FWM process is phase matched over a broad range of frequencies, thus giving broadband noise amplification. Our analysis is performed entirely in the frequency domain, and we take into account the stochastic nature of the noise field as well as fiber loss and dispersion to any order. In Section 3 a simple differential equation is derived that describes catastrophic noise buildup. In the case of short fibers, for which fiber loss can be neglected, a simple analytical solution is derived for the gain of this process. In Section 3 we describe the experimental setup and present our observations, which are compared with numerical results from the model developed in Section 2 as well as with those from the NLSE. We complete our study of this effect by simulating long amplified links for which the effect of random fluctuations of $\nu_0 = c/\lambda_0$ along the fiber is considered. Finally, in Section 4 we draw our conclusions and discuss possible implications for DWDM systems.

2. THEORY: FOUR-WAVE MIXING AND PHASE MATCHING

FWM involving ASE noise differs from that which involves just lasers (coherent sources) in that the statistical

nature of the noise field has to be taken into account. We consider two strong lasers with frequencies ω_1 and ω_2 and input powers P_{01} and P_{02}, respectively, interacting with a background ASE field, $E(z,t)$ (z is the position along the fiber, and t is time). At the fiber input ($z = 0$) we assume that $E(0,t)$ is a stationary random process, so the ensemble average of its Fourier transform satisfies

$$\langle E_0(\omega) E^*(0,\omega')\rangle = \text{const.} \times N_0(\omega)\delta(\omega - \omega'), \quad (1)$$

where ω is the frequency, $N_0(\omega)$ is the noise input power spectrum, $\delta(\omega)$ is Dirac's delta function, and the superscript * denotes a complex conjugate.

We write the field of a monochromatic laser at frequency ω_n $(n = 1,2)$ as $E_{\text{laser}\,n}(z,\omega) = \pi E_n(z)\delta(\omega - \omega_n) + \pi E_{-n}(z)\delta(\omega - \omega_{-n})$, where $E_{-n} = E_n^*$ and $\omega_{-n} = -\omega_n$. The total field in our problem is $E_{\text{laser1}} + E_{\text{laser2}} + E$, where E is the noise field ($|E| \ll |E_{\text{laser1,2}}|$). The propagation equation, in the frequency domain, is[13]

$$\left[\frac{\partial^2}{\partial z^2} + k^2(\omega)\right]E(z,\omega) = -\frac{3\omega^2}{4c^2}\sum_{jk}\chi_{jk}^{(3)}E_j(z)E_k(z)E(z,\omega_{jk}), \quad (2)$$

where $k(\omega) = \beta(\omega) - i\alpha/2$, $\beta(\omega)$ is the wave vector at ω, α is the attenuation coefficient, $\chi_{jk}^{(3)} = \chi^{(3)}(\omega;\omega_j,\omega_k,\omega_{jk})$, and $\omega_{jk} = \omega - \omega_j - \omega_k$ $(j,k = \pm 1, \pm 2)$. Equation (2) follows directly from the definition of the third-order nonlinear polarization[13] where we have retained only terms that are linear in the noise field. We have assumed also that the total field is linearly polarized, thus allowing us to disregard the tensorial nature of $\chi^{(3)}$. We define the spatially slowly varying amplitudes for the noise and the lasers: $\tilde{A}(z,\omega) = E(z,\omega)\exp[i\beta(\omega)z + \alpha z/2]$ and $\tilde{A}_n(z) = E_n(z)\exp[ik(\omega_n)z - i\phi_n(z,\omega_n)]$, where $\phi_1 = \phi_1(0) - \gamma(P_{01} + 2P_{02})[1 - \exp(-\alpha z)]/\alpha$ and $\phi_2 = \phi_2(0) - \gamma(P_{02} + 2P_{01})[1 - \exp(-\alpha z)]/\alpha$, where $\phi_n(0)$ represents the initial ($z = 0$) phase of the corresponding laser and γ is the nonlinear coefficient $\gamma(\omega) = 3\omega\chi^{(3)}/4c^2\varepsilon_0 n_0^2 A_{\text{eff}}$ (A_{eff} is the effective cross-sectional area of the fiber, c is the speed of light in vacuum, n_0 is the linear refractive index, and ε_0 is the electrical permittivity of vacuum). Amplitude $\tilde{A}_n(z)$ is related to laser power $P_n(z)$ by the expression $P_n(z) = 1/2\varepsilon_0 n_0 c|\tilde{A}_n(z)|^2\exp(-\alpha z)A_{\text{eff}}$.

The propagation equation [Eq. (2)] for the noise at frequency ω becomes

$$\begin{aligned}\frac{\partial}{\partial z}\tilde{A}(z,\omega) = {} & -i\gamma\{2(P_1 + P_2)\tilde{A}(z,\omega) \\ & + P_1\exp(i\Delta\beta_a z + i2\phi_1)\tilde{A}^*(z, 2\omega_1 - \omega) \\ & + P_2\exp(i\Delta\beta_b z + i2\phi_2)\tilde{A}^*(z, 2\omega_2 - \omega) \\ & + 2\sqrt{P_1P_2}\exp[i\Delta\beta_c z \\ & + i(\phi_1 - \phi_2)]\tilde{A}(z, \omega_2 - \omega_1 + \omega) \\ & + 2\sqrt{P_1P_2}\exp[i\Delta\beta_d z \\ & + i(\phi_2 - \phi_1)]\tilde{A}(z, \omega_1 - \omega_2 + \omega) \\ & + 2\sqrt{P_1P_2}\exp[i\Delta\beta_e z \\ & + i(\phi_1 + \phi_2)]\tilde{A}^*(z, \omega_1 + \omega_2 - \omega)\}, \quad (3)\end{aligned}$$

In deriving Eq. (3) we neglected the small frequency dependence in α and γ and assumed that $\tilde{A}$ is a slowly varying function of z ($|\partial^2\tilde{A}/\partial z^2| \ll |\beta\partial\tilde{A}/\partial z|$) and $\beta(\omega) \gg \alpha$. We also assumed that the pump lasers are not depleted by the nonlinear interactions, so the attenuation is given by $P_n(z) = P_{0n}\exp(-\alpha z)$.

In Eq. (3) we have the wave-vector mismatches introduced by dispersion:

$$\Delta\beta_a = \beta(\omega) + \beta(2\omega_1 - \omega) - 2\beta(\omega_1), \quad (4a)$$

$$\Delta\beta_b = \beta(\omega) + \beta(2\omega_2 - \omega) - 2\beta(\omega_2), \quad (4b)$$

$$\Delta\beta_c = \beta(\omega) - \beta(\omega_2 - \omega_1 + \omega) + \beta(\omega_2 - \beta(\omega_1), \quad (4c)$$

$$\Delta\beta_d = \beta(\omega) - \beta(\omega_1 - \omega_2 + \omega) + \beta(\omega_1) - \beta(\omega_2), \quad (4d)$$

$$\Delta\beta_e = \beta(\omega) + \beta(\omega_1 + \omega_2 - \omega) - \beta(\omega_1) - \beta(\omega_2). \quad (4e)$$

Equation (3) has six terms on its right-hand side that account for nonlinear interactions between two lasers and the background noise. The first term can be interpreted as cross-phase modulation, although, rigorously speaking, cross-phase modulation is introduced in the time domain, whereas Eq. (3) is in the frequency domain. The remaining five terms represent five FWM processes that contribute to the noise field at a given frequency ω. These processes, designated in the same order as the element of Eqs. (4), are FWM (a) between laser 1 and noise at $\omega_a = 2\omega_1 - \omega$, making a contribution at ω via $2\omega_1 - \omega_a = \omega$; (b) between laser 2 and noise at $\omega_b = 2\omega_2 - \omega$ (through $2\omega_2 - \omega_b = \omega$); and between the two lasers and noise at (c) $\omega_c = \omega_2 - \omega_1 + \omega$ or (d) $\omega_d = \omega_1 - \omega_2 + \omega$ and (e) $\omega' = \omega_1 + \omega_2 - \omega$ ($\omega = \omega_1 + \omega_2 - \omega'$). In this paper we consider the case when the laser frequencies are chosen such that the condition $\omega_1 + \omega_2 = 2\omega_0$ is nearly satisfied. We show below that, for this condition, only process (e) is wave-vector matched over a broad range of frequencies. In what follows, we limit our analysis to FWM process (e) and disregard all other processes.

In process (e), a noise Fourier component at an arbitrary frequency ω is coupled to another component at $\omega' = \omega_1 + \omega_2 - \omega$ (see Fig. 1). To study this process we re-

tain, on the right-hand side of Eq. (3), only the first and last terms. We further define $A = \tilde{A}(z, \omega)\exp\{2i(P_{01} + P_{02})[1 - \exp(-\alpha z)]/\alpha\}$. This definition results in the following set of coupled equations:

$$\frac{\partial A}{\partial z} = aA'^*, \quad \frac{\partial A'}{\partial z} = aA^*, \tag{5}$$

where $A' = A(z, \omega_1 + \omega_2 - \omega)$,

$$a = -2i\gamma\sqrt{P_1 P_2}\exp(i\Delta\beta z + i\phi), \tag{6}$$

$\Delta\beta = \Delta\beta_e$, and $\phi = \phi_1(0) + \phi_2(0) + \gamma(P_{01} + P_{02})[1 - \exp(-\alpha z)]/\alpha$.

Coupled equations (5) can easily be decoupled, yielding

$$\left(\frac{\partial^2}{\partial z^2} + b\frac{\partial}{\partial z} - |a|^2\right)A = 0, \tag{7}$$

where $b = -(\partial \ln a/\partial z) = \alpha - i[\Delta\beta + \gamma(P_1 + P_2)]$. Equation (7) is the main theoretical result of our analysis and describes the fundamentals of noise–signal interaction for the FWM process considered. It is shown below that $\Delta\beta$ is symmetrical relative to the interchange of ω and ω', with the consequence that Eq. (7) is also satisfied by A' with the same coefficients b and $|a|^2$. In general, Eq. (7) cannot be integrated analytically because $|a|^2$ and b are functions of z. However, Eq. (7) is a linear second-order differential equation, and its solution can be written as a linear combination of the initial values of $A[A(0, \omega) = E(0, \omega)]$ and its first derivative, which, from Eqs. (5), is given by $\partial A(0, \omega)/\partial z = a(0)E^*(0, \omega')$:

$$A(z, \omega) = F(z, \omega)E(0, \omega) + H(z, \omega)E^*(0, \omega'), \tag{8}$$

where F and H are deterministic functions of position and frequency that do not depend on the details of the random process that describes the input noise field. It is shown in Appendix A that F and H both satisfy our fundamental Eq. (7). However, the advantage of working with F and H (instead of with A and A') is that these functions are deterministic, whereas A and A' are stochastic. The output power spectrum, $N(\omega)$, is proportional to $\langle|E(L, \omega)|^2\rangle = \langle|A(L, \omega)|^2\rangle\exp(-\alpha L)$, and, using Eqs. (1) and (8), we obtain

$$N(\omega) = |F(L, \omega)|^2\exp(-\alpha L)N_0(\omega) + |H(L, \omega)|^2\exp(-\alpha L)N_0(\omega'). \tag{9}$$

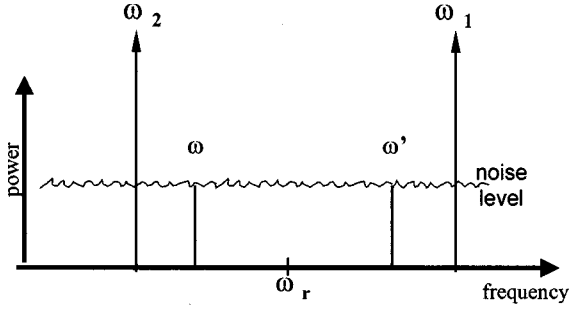

Fig. 1. Two monochromatic lasers interacting with background ASE noise. Spectral components at ω and ω', symmetrically located relative to $\omega_r = (\omega_1 + \omega_2)/2$, are coupled to each other by FWM processes $\omega_1 + \omega_2 - \omega' = \omega$ and $\omega_1 + \omega_2 - \omega = \omega'$. If $\omega_r = \omega_0$ (the zero-dispersion frequency of the fiber), these processes are phase matched up to third-order dispersion.

Equation (9) expresses the output spectrum as a function of the input. One can see that the output power spectrum depends on the input powers at ω and at $\omega' = \omega_1 + \omega_2 - \omega$. With fiber loss neglected ($\alpha = 0$), these functions can be calculated analytically (see below). For $\alpha \neq 0$, F and H must be obtained numerically, and we show, in Appendix A, an efficient algorithm for this purpose.

When $\alpha = 0$, coefficients $|a|^2$ and b are constants and Eq. (7) can be readily solved. The solution can be expressed as

$$N(\omega) = 16\gamma^2 P_{01}P_{02}\frac{\sinh^2(gL/2)}{g^2} \times [N_0(\omega') + N_0(\omega)] + N_0(\omega), \tag{10a}$$

$$g = [-\Delta\beta^2 - 2\gamma\Delta\beta(P_{01} + P_{02}) - \gamma^2(P_{01} + P_{02})^2 + 16\gamma^2 P_{01}P_{02}]^{1/2}. \tag{10b}$$

It is interesting to note that this solution is similar to that derived in Ref. 14. In that paper the catastrophic noise amplification is treated theoretically for the case of a single laser interacting with noise [equivalent to our processes (a) or (b) in Eqs. (3) above]. Furthermore, the gain coefficient [Eq. (10b)] is identical to that obtained for a two-pump fiber-optic parametric amplifier,[15] which is reasonable because the underlying FWM processes are the same, irrespective of whether a signal or noise is being amplified. It is not obvious, though, that such a parametric amplifier should give the same black-box gain for a weak laser signal or noise, given the different natures of stochastic and deterministic fields. In fact, an important difference should be noted: the output noise power at ω depends on the input at ω', yielding a gain factor that, for $N_0(\omega') \approx N_0(\omega)$, is roughly twice as large as that of the signal. Strictly speaking, the problem considered here should be compared with that of a parametric amplifier for which the idler at ω' is already present at the fiber input with an amplitude that is comparable with that of the signal. As was pointed out in Refs. 3 and 16, which treated the single-pump case, signal amplification depends strongly on the initial phase relationship among the pump, the signal, and the idler. That phase sensitivity of the parametric amplifiers arises from interference among the interacting waves. In the present problem of noise amplification, there is no such phase dependence because noise components at different frequencies are uncorrelated [see Eq. (1)] and do not interfere.

We now describe the derivation of $\Delta\beta$ that gives wave-vector matching over a large bandwidth. In terms of the coefficients of a Taylor expansion of wave vector $\beta(\omega)$ about an arbitrary reference frequency ω_r,[15] we have that $\Delta\beta = \Delta\beta_2 + \Delta\beta_3 + \ldots$, where $\Delta\beta_2$ is the mismatch that is due to second-order dispersion, and so on. If we choose $\omega_r = (\omega_1 + \omega_2)/2$, then

$$\Delta\beta_n = \frac{1 + (-1)^n}{n!}\beta_n(\omega_r)[(\omega - \omega_r)^n - (\omega_1 - \omega_r)^n], \tag{11}$$

with $\beta_n(\omega_r) = \partial^n\beta/\partial\omega^n|_{\omega_r}$. Equation (11) shows that all odd terms are identically zero. If we further make ω_r co-

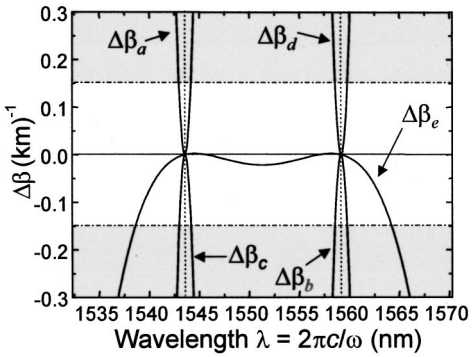

Fig. 2. Wave-vector mismatch for the five possible FWM processes that involve two lasers (symmetrically tuned relative to ω_0) and noise. The lasers' wavelengths are indicated by dotted lines.

incident with the zero-dispersion frequency, $\omega_r = \omega_0 = 2\pi c/\lambda_0$, then $\beta_2(\omega_r) = 0$, and the lowest-order dispersion contribution to phase mismatch is given by fourth-order dispersion:

$$\Delta\beta = \Delta\beta_4 + \Delta\beta_6 + \ldots . \tag{12}$$

Then FWM combinations of the type $\omega_1 + \omega_2 - \omega = \omega'$ and $\omega_1 + \omega_2 - \omega' = \omega$ provide quasi-phase-matched mechanisms to amplify, simultaneously, spectral components of noise at ω and ω' (see Fig. 1). Retaining only terms to fourth order [see Eqs. (11) and (12)], we have that

$$\Delta\beta = \Delta\beta_4 = (1/12)\beta_4(\omega_r)[(\omega - \omega_r)^4 - (\omega_1 - \omega_r)^4]. \tag{13}$$

Rigorously speaking, $\Delta\beta = 0$ is not quite the phase-matching condition. A general trend in Eqs. (5) is that the increasing rate of the noise field will be maximum when the driving term has a stationary phase, i.e., when $\Delta\beta_{\text{Total}} = \Delta\beta + \partial\phi/\partial z \approx 0$. A nonlinear contribution $(\partial\phi/\partial z)$, which in some cases can be important, is added to the dispersion contribution. The result expresses a power-dependent phase-matching condition,[3] and the lasers at ω_1 and ω_2 will be slightly asymmetrical relative to ω_0 for exact wave-vector matching.

In dispersion-shifted fibers, efficient FWM interaction with noise can occur over a large bandwidth for a process of the type of $\omega_1 + \omega_2 - \omega' = \omega$ when the lasers at ω_1 and ω_2 are symmetrically tuned relative to ω_0. The mismatch of FWM processes (a)–(d) cannot be small over a large bandwidth. This fact is illustrated in Fig. 2, where $\Delta\beta$ for all FWM processes is plotted. Figure 2 was generated with the assumption that $\omega_1 - \omega_0 = \omega_0 - \omega_2$ (the laser wavelengths are indicated by the dotted lines), $\beta_3 = 0.11\,\text{ps}^3/\text{km}$, and $\beta_4 = -0.00039\,\text{ps}^4/\text{km}$ (see Section 3 below for calculations of β_3 and β_4). A given FWM process is efficient over the range of frequencies at which the phase mismatch $|\Delta\beta L_{\text{eff}}| < \pi$ {where the effective fiber length is $L_{\text{eff}} = [1 - \exp(-\alpha L)]/\alpha$}. In long fibers, $L_{\text{eff}} \approx 1/\alpha$ is typically 20 km. Thus, typically, the bandwidth for FWM is determined by $|\Delta\beta| < \pi/L_{\text{eff}} \sim 0.15\,\text{km}^{-1}$. This region is indicated in Fig. 2 by the nonshadowed area. We can see from Fig. 2 that process (e) has a bandwidth of ~20 nm, whereas all other processes (a–d) have bandwidths that are smaller than 2 nm.

3. EXPERIMENTS

The experimental setup is shown in Fig. 3. We used a dispersion-shifted fiber with $L = 25\,\text{km}$, $\alpha = 0.05\,\text{km}^{-1}$, $\lambda_0 = 1551.35\,\text{nm}$, $S_0 = 0.073\,(\text{ps/nm}^2)/\text{km}$ [$S_0 = (2\pi c/\lambda_0^2)^2\beta_3(\omega_0)$ is the dispersion slope at λ_0] and $\gamma = 2.3\ \text{W}^{-1}/\text{km}$. All these parameters were measured by either optical time-domain reflectometry (for α and L) or the modulational-instability-based method described in Ref. 17. Two cw tunable external-cavity lasers, with wavelengths λ_1 and λ_2 ($\lambda_1 < \lambda_0 < \lambda_2$), were spectrally broadened by 400-MHz phase modulation to prevent stimulated Brillouin scattering in the fiber and were amplified to $P_{01} \cong P_{02} \cong 18\,\text{dBm}$ by two cascaded erbium-doped fiber amplifiers (EDFAs). Using two EDFAs allowed us to control the shape of the noise spectrum and to study the simplest case of almost flat input noise. We used a 2×2 coupler to monitor the input spectrum (10% port) and the Brillouin backscattering. The frequency and the amplitude of the electrical signal driving the phase modulator were adjusted to eliminate Brillouin backscattering (<40 dB). Spectra were recorded with an optical spectrum analyzer that had a 0.1-nm resolution bandwidth.

In our model we assumed that both lasers and noise fields had linear polarization and were parallel to one another. In the experiment, however, the input ASE was unpolarized and the lasers evolved into an elliptical polarization owing to fiber birefringence. We experimentally analyzed the dependence of noise gain on polarization. To this end, we added a polarization controller and a polarizer at the fiber output and adjusted the controller to render the output lasers nearly linearly polarized and oriented parallel or perpendicular to the axis of the polarizer. It was not possible to obtain perfect linear polarization for both lasers simultaneously, as birefringence depends on wavelength. Using this procedure, though, we could measure the output ASE polarized roughly parallel or perpendicular to the lasers. The gain ratio for parallel ($G_\parallel$) and perpendicular ($G_\perp$) states, for $G_\parallel = 16\,\text{dB}$, was measured to be ~10 dB in the spectral region near λ_0. This is in agreement with the expected result for an ideal fiber without birefringence, for which the effective third-order susceptibility when the noise field is polarized orthogonally to the lasers is one third of that for the parallel case [$\chi^{(3)}_{yxxy} = \chi^{(3)}_{xxxx}/3$].

In Fig. 4(a) we show the input and output spectra when the lasers were tuned at $\lambda_1 = 1543.5$ and $\lambda_2 = 1559.2\,\text{nm}$, i.e., nearly symmetrical relative to λ_0.

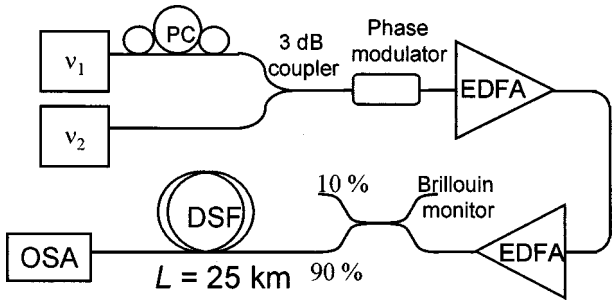

Fig. 3. Experimental setup: PC, polarization controller; OSA, optical spectrum analyzer; DSF, dispersion-shifted fiber.

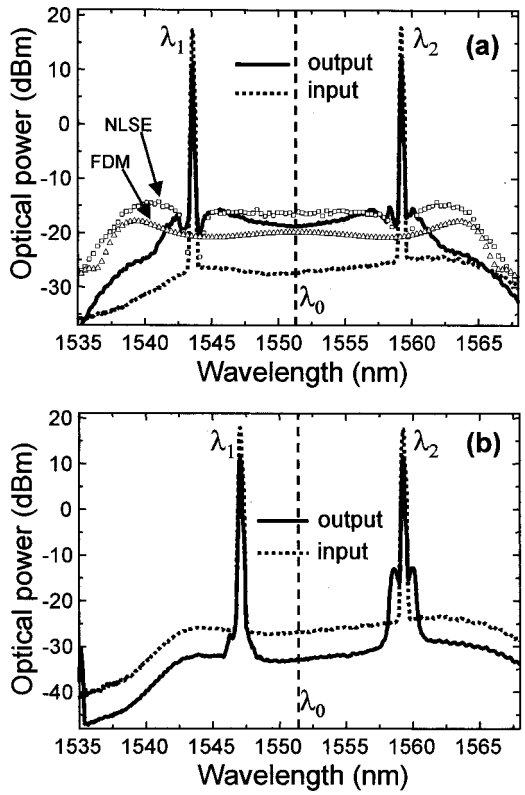

Fig. 4. Input and output spectra with $P_{01} = P_{02} \sim 18.3$ dBm and for λ_1 and λ_2 located (a) symmetrically or (b) asymmetrically relative to the zero-dispersion wavelength. In (b) λ_2 was tuned ~2.5 nm from symmetry.

We observe that the output ASE level is larger than at the input by ~10 dB over the whole spectral region between the lasers. Considering that the fiber and the connectors provided a total loss of ~6 dB, the FWM gain for noise was ~16 dB in this case. As can be observed from this figure, large gain occurs mainly for noise Fourier components located from ω_1 to ω_2. This fact is related to the form of the wave-vector mismatch ($\Delta\beta_c$) spectrum plotted in Fig. 2.

We also show, in the same figure, the simulations performed with our model, the frequency-domain model (FDM), and by solution of the NLSE, both with the same parameters as were used in the experiment. We performed all the simulations assuming a flat input noise spectrum. Compared with the experimental spectrum, the FDM yields a smaller gain for the innermost frequencies and a larger gain for the outermost ones, whereas the NLSE gives a larger gain for the entire spectrum, with larger discrepancies for the outermost frequencies. With numerical experiments that used the FDM or the NLSE, we verified that the larger gain for the outermost frequencies is due to the fact that we considered λ_0 constant along the 25 km of fiber. It is shown below that varying λ_0 along the fiber causes the symmetry to be partially lost, thus strongly reducing the gain for the outermost frequencies.

The advantage of the FDM compared with the NLSE for simulations of laser–noise interactions is that the FDM calculates deterministic functions (F and H); the stochastic noise field is included by the input spectral density $N(0, \omega)$ at the end of the calculus. In the NLSE simulations the input noise field is randomly generated, and we must take tens of thousands of points for a realistic description of the stochastic process. Furthermore, each execution of the NLSE program represents the nonlinear response of the fiber to a single outcome of this random process, and, at high pump powers, it is necessary to average the output from 30 or more simulations. Thus, for the pump powers considered in this paper, a typical FDM simulation requires 1 min for execution, whereas the NLSE program requires ~5 h on the same computer. The FDM program is useful for testing hypotheses and getting quick answers but does not compare in accuracy with the NLSE program. The FDM is particularly useful for evaluating the contribution of a given FWM process isolated from the others. The NLSE program correctly accounts for all other laser–noise FWM interactions as well as laser–laser FWM and even cascaded FWM processes that develop along the fiber, but it does not provide physical insights into which particular process is responsible for each feature in the output spectrum.

Detuning λ_1 by 2.5 nm (~0.315 THz) from the previous symmetric case, we observe [Fig. 4(b)] that the experimental FWM gain is reduced to ~0.5 dB. This clearly shows that the catastrophic noise amplification is highly sensitive to detuning, as predicted from the wave-vector matching analysis.

In the numerical simulations we used $\beta_4(\omega_0) = -0.00039\ \mathrm{ps}^4/\mathrm{km}$. We obtained this value by considering that, near the zero-dispersion wavelength, the dispersion parameter can be expressed as $D(\lambda) = S_0\lambda(1 - \lambda_0^3/\lambda^3)/3$. Writing this dispersion relation as a function of ω and expanding in power series of $\omega - \omega_0$, we obtained $\beta_3 = \partial\beta_2/\partial\omega$ and $\beta_4 = \partial\beta_3/\partial\omega$, where $\beta_2 = -\lambda^2 D/2\pi c = -(2\pi c)^2 S_0(1/\omega^3 - 1/\omega_0^3)/3$. Substituting the average measured values into our fiber, $\lambda_0 = 1551.35$ nm and $S_0 = 0.073\ (\mathrm{ps/nm}^2)/\mathrm{km}$, we obtained $\beta_3(\omega_0) = 0.11\ \mathrm{ps}^3/\mathrm{km}$ and $\beta_4(\omega_0) = -3.9 \times 10^{-4}\ \mathrm{ps}^4/\mathrm{km}$.

In Fig. 5 we show the FWM gain at $\lambda = \lambda_0$ for the symmetrical case as a function of input power ($P_{01} = P_{02}$) as obtained from FDM numerical calculations and measurements, with the same parameters and laser wavelengths used in Fig. 4(a). At large input laser powers, the FWM gain should saturate as a result of pump depletion. Our data in Fig. 5 indicate that, up to the maximum power

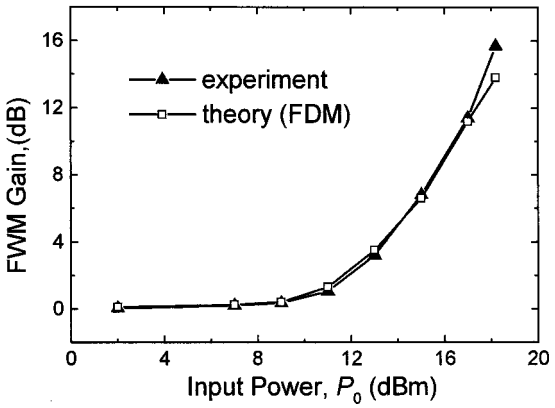

Fig. 5. FWM gain as a function of input power $P_{01} = P_{02} = P$.

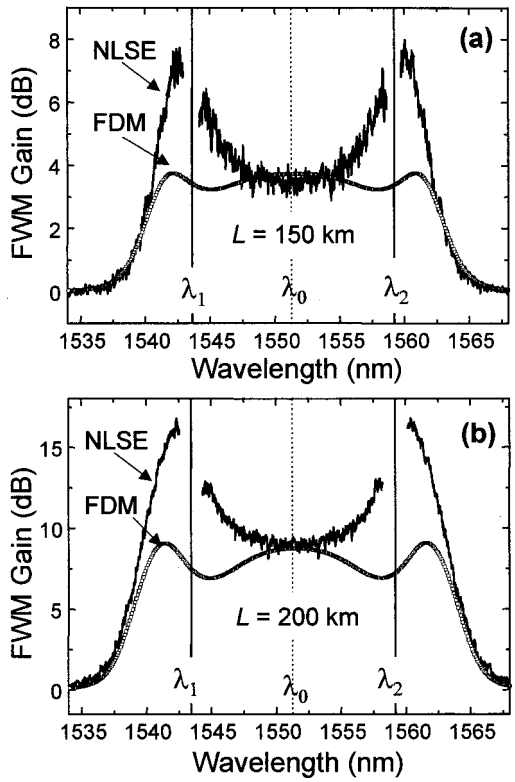

Fig. 6. Simulated FWM gain spectra with $\lambda_1 \sim 1543.5$ nm and $\lambda_2 = 1559.2$ nm for (a) $P_{01} = P_{02} = 15$ mW and (b) $P_{01} = P_{02} = 30$ mW.

that we could obtain in the experiment, we did not see saturation. The agreement between experiments and FDM is quite good, except at 18.3-dBm input power, where the measured gain is larger than the calculated gain. An explanation for this discrepancy could be found in cascaded FWM processes that are not included in the FDM.

We now turn our attention to the study of longer links without in-line amplifiers. We simulated two links, with $L = 150$ km [Fig. 6(a)] and $L = 200$ km [Fig. 6(b)] with input peak powers of 15 and 30 mW, respectively, which were sufficient to overcome these distances. The two lasers were nearly symmetrically located relative to ν_0, with the same values of λ_1 and λ_2 that we used for Fig. 4(a). We observed FWM gains of ~4 and ~8.5 dB, respectively, over a bandwidth of ~22 nm. For comparison, we plotted our results by solving the NLSE. For noise frequencies near the laser frequencies, where FWM processes (a)–(d) are wave-vector matched, the NLSE simulations showed more gain than for our FDM when only FWM process (e) was considered. The FDM tends to underestimate the gain and gives a spectral shape that reminds one of the form of $\Delta\beta$ for process (e) (see Fig. 2).

We now consider long links with in-line amplifiers. In Fig. 7(a) we simulate a link of $L = 400$ km with three in-line amplifiers (100 km between consecutive amplifiers) with flat gain and with uncorrelated noise added at each amplifier stage. The input power was $P_{01} = P_{02} = 10$ mW, and the lasers were tuned to the same wavelengths as for Fig. 6. We define the normalized gain as the noise amplification that is due to nonlinear effects; i.e., the 0-dB level is the output noise level in the absence of nonlinearity. The normalized gain for this case is ~4.5 dB over a bandwidth of 22 nm. For the longer links of $L = 1000$ km that comprise nine amplifiers, the normalized gain is ~11 dB over the same bandwidth. These simulations, which use input power levels that are typical in transmission systems but with a constant zero-dispersion wavelength along all the fibers in the link, predict large noise buildup. It is well known, however, that, in an actual fiber, λ_0 varies randomly along the fiber.[18]

To investigate the influence of λ_0 fluctuations, we simulated a link of $L = 400$ km (with in-line amplifiers every 100 km), modeling the λ_0 variation as $\lambda_0(z) = \langle\lambda_0\rangle + \Delta\lambda_0(z) + \delta\lambda_0(z)$, where $\langle\lambda_0\rangle = 1551.35$ nm for all simulations. $\delta\lambda_0(z)$ is a rapidly varying fluctuation (zero correlation length) modeled as a Gaussian process with zero mean and a standard deviation of 0.2 nm. Finally, $\Delta\lambda_0(z)$ is a slow fluctuation modeled as a constant value for every 4-km segment and varies randomly from segment to segment as a Gaussian process with zero mean and a 10-nm standard deviation.

In Fig. 8(a) we have plotted our results. The normalized gain is now ~1.8 dB and should be compared with the 4.5 dB obtained for Fig. 7(a). This decrease in noise amplification is due to fluctuations in λ_0. Nevertheless, the spectral shape is roughly the same as in the case without λ_0 fluctuations. Now we detune laser 2 slightly, by $\Delta = 0.1$ nm [$\Delta = |\langle\lambda_0\rangle - (\lambda_1 + \lambda_2)/2|$], and the spec-

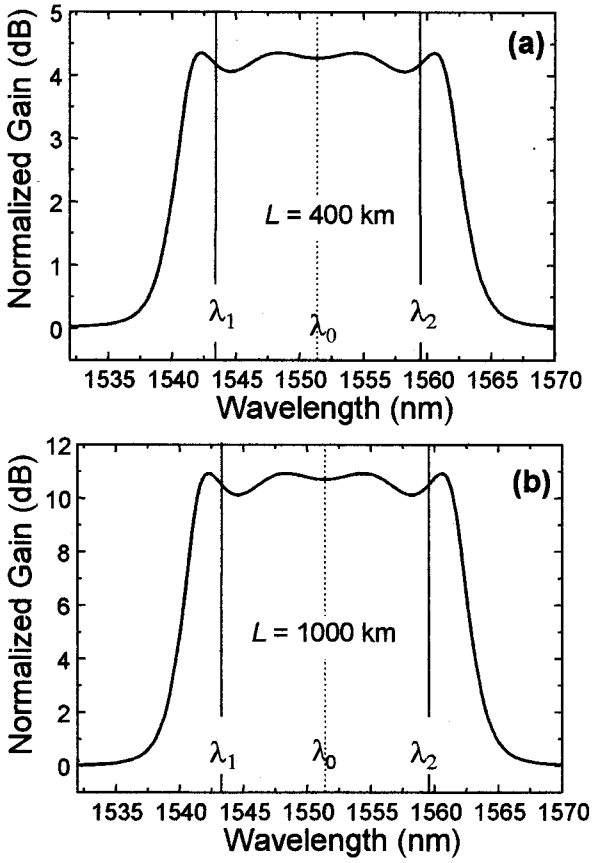

Fig. 7. Simulated FWM gain spectra with $\lambda_1 \sim 1543.5$ nm and $\lambda_2 = 1559.2$ nm with $P_{01} = P_{02} = 10$ mW.

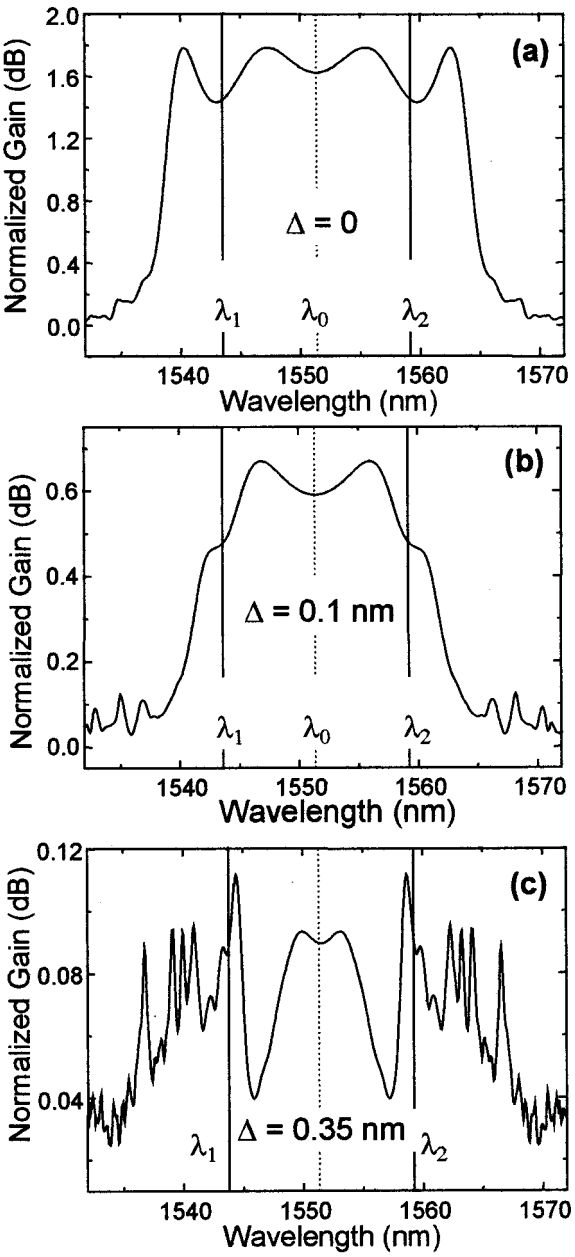

Fig. 8. Simulated FWM gain spectra with $\lambda_1 \sim 1543.5$ nm and $\lambda_2 = 1559.2$ nm with $P_{01} = P_{02} = 10$ mW for $L = 1000$ km.

trum is as shown in Fig. 8(b). The normalized gain now drops to ~0.7 dB over a bandwidth of 15 nm, and for a detuning of $\Delta = 0.35$ nm (~45 GHz) the gain is 0.1 dB and the spectral shape changes sharply. These results indicate that (1) fluctuations of λ_0 tend to reduce gain but preserve the gain spectral shape, with the important conclusion that, essentially, the gain bandwidth is limited by fourth-order dispersion and slow fluctuations, and (2) small detunings of the pump wavelengths considerably reduce the efficiency of this FWM process.

4. CONCLUSIONS

In conclusion, we have investigated four-wave mixing between two lasers and noise near the zero-dispersion frequency of optical fibers. In general, several FWM processes that involve one or both lasers can occur. However, when the lasers are tuned symmetrically relative to the zero-dispersion frequency, a particular FWM process becomes phase matched up to third-order dispersion and dominates. This process leads to catastrophic noise buildup over a broad spectral range. We have developed a simple model for this process that takes into account the stochastic nature of the ASE field, dispersion to any order, and fiber loss. All details are contained in a simple differential equation [Eq. (6)], which has an analytical solution for lossless fibers. Experiments have validated the essence of our model. For the fiber and laser power used in our experiments, ASE spectral components within a ~22-nm bandwidth near λ_0 are efficiently amplified up to 10 dB (to 16 dB if we discount fiber loss), in good agreement with our model. In an ideal fiber, with no fluctuations of λ_0 along the fiber length, the bandwidth of this process is limited by fourth-order dispersion. When λ_0 fluctuations are considered, the efficiency is reduced, but, for realistic modeling of this fluctuation in typical fibers, the spectral shape is essentially preserved. The efficiency depends strongly on the detuning of one the lasers from the symmetric condition. Our investigations with two lasers have indicated that noise amplification will be important whenever the average frequency of any two channels of a DWDM system coincides with λ_0 within a certain tolerance (45 GHz in the case of our fiber). The conditions for catastrophic noise amplification depend on the optical power, dispersion, and fluctuations of λ_0 along the fiber but are likely to be met in long-haul DWDM systems operating near λ_0 with a channel spacing of 100 GHz or less.

APPENDIX A

As established in Eq. (7), we can write the spatially slowly varying stochastic field in the frequency domain as $A(z, \omega) = FE(0, \omega) + HE^*(0, \omega')$. Substituting this expression into Eqs. (5) gives $(\partial F/\partial z) = aH^*$ and $(\partial H/\partial z) = aF^*$, which can be decoupled to yield

$$\left(\frac{\partial^2}{\partial z^2} + b\frac{\partial}{\partial z} - |a|^2\right)F = 0. \tag{A1}$$

Equation (A1), which coincides with Eq. (7) for A, is also satisfied by H. The initial conditions for solving Eq. (A1) are that $F(0, \omega) = 1$ and $\partial F(0, \omega)/\partial z = 0$.

In a numerical resolution, we divide the fiber into N segments of length $\Delta z = L/N$, where we take b and $|a|^2$ as constant coefficients: $\bar{b} = \alpha - i[\Delta\beta + \gamma(\overline{P_1 + P_2})]$, where $\overline{P_1 + P_2}$ is the average power in each segment and $\overline{|a|^2} = \gamma^2\overline{P_1 P_2}$. With constant coefficients, Eq. (A1) is a linear, second-order differential equation in each segment of fiber. The solution, at each end of a segment, can be expressed as a linear combination of the initial values of F and $\partial F/\partial z$ in that segment. But, inasmuch as $\partial F/\partial z = aH^*$, we write

$$\begin{bmatrix} F(z + \Delta z, \omega) \\ H(z + \Delta z, \omega') \end{bmatrix} = \mathbf{T}(z)\begin{bmatrix} F(z, \omega) \\ H(z, \omega') \end{bmatrix}, \tag{A2}$$

$$\mathbf{T}(z) = \begin{bmatrix} T_{11}(z) & T_{12}(z) \\ T_{12}^*(z) & T_{11}^*(z) \end{bmatrix}, \tag{A3}$$

where

$$T_{11} = \frac{\lambda_- \exp(\lambda_+ \Delta z) - \lambda_+ \exp(\lambda_- \Delta z)}{\lambda_- - \lambda_+}, \tag{A4}$$

$$T_{12} = a(z) \frac{\exp(\lambda_+ \Delta z) - \exp(\lambda_- \Delta z)}{\lambda_- - \lambda_+}, \tag{A5a}$$

$$\lambda_\pm = 1/2[-\bar{b} \pm (\bar{b}^2 + 4|a|^2)^{1/2}]. \tag{A5b}$$

The solution to Eq. (A1) is then a simple product of matrices:

$$\begin{bmatrix} F(L, \omega) \\ H(L, \omega') \end{bmatrix} = T_{N-1} \ldots T_1 T_0 \begin{bmatrix} 1 \\ 0 \end{bmatrix}, \tag{A6}$$

where $\mathbf{T}_n = \mathbf{T}(n\Delta z)$ $(n = 0, \ldots, N-1)$. It is not necessary to take segments of equal lengths, but, for good accuracy, the fiber steps should be maintained as $\Delta z \ll 1/|a|$. In the numerical simulations for $L = 25$ km and $P_{01} = P_{02} = 18$ dBm, we used a constant step of 12.5 m.

APPENDIX B

A more convenient input–output relation can be derived if we note that, from Eqs. (5), $\partial(|A|^2 - |A'|^2)/\partial z = 0$, which implies that the difference

$$\langle |A(z, \omega)|^2 \rangle - \langle |A(z, \omega')|^2 \rangle = N_0(\omega) - N_0(\omega') \tag{B1}$$

remains constant during propagation. Substituting Eq. (B1) into Eq. (8), we obtain

$$R(\omega) \equiv \frac{N(\omega) - N_0(\omega)\exp(-\alpha L)}{1/2[N_0(\omega) + N_0(\omega')]\exp(-\alpha L)} = |F|^2 + |H|^2 - 1. \tag{B2}$$

Note that $N_0(\omega)\exp(-\alpha L)$ is the measured output spectrum in the absence of FWM coupling. In general, an input asymmetric spectrum $N_0(\omega)$ produces an asymmetric output $N(\omega)$. However, Eq. (B2) states that the difference between pump on and pump off outputs at ω, normalized to the pump-off mean of outputs at ω and ω', is independent of noise spectral asymmetries at the input of the fiber. This makes the ratio $R(\omega)$ convenient to use for comparisons of theory and experiment. All terms that define $R(\omega)$ in Eq. (B2) are easily measured, whereas functions $F(L, \omega)$ and $H(L, \omega)$ can be calculated.

For the special case of $\alpha = 0$, $R(\omega)$ is given by

$$R(\omega) = 32\gamma^2 P_{01} P_{02} \frac{\sinh^2(gL/2)}{g^2}, \tag{B3}$$

where g is as defined in Eq. (10b).

ACKNOWLEDGMENTS

This study was supported by the Research and Development Center, Ericsson Telecomunicações S. A., Brazil. We thank Xtal Fibras Ópticas and Corning, Inc., for donations of fibers that were used in the experiments. This study was partially supported by the Brazilian funding agencies Fundação de Amparo à Pesquisa do Estado de São Paulo, Progama de Apoio aos Núcleos de Excelência, Coordenação de Aperfieçoamento de Pessoal de Nível Superior, and Conselho Nacional de Desenvolvimento Científico e Tecnológico.

J. M. Chávez Boggio's e-mail address is jmchavez@ifi.unicamp.br.

REFERENCES

1. R. W. Tkach, A. R. Chraplyvy, F. Forghieri, A. H. Gnauck, and R. M. Derosier, "Four-photon mixing and high-speed WDM systems," J. Lightwave Technol. **13**, 841–849 (1995).
2. D. Marcuse, A. R. Chraplyvy, and R. W. Tkach, "Effect of fiber nonlinearity on long-distance transmission," J. Lightwave Technol. **9**, 121–128 (1991).
3. R. H. Stolen and J. E. Bjorkholm, "Parametric amplification and frequency conversion in optical fibers," IEEE J. Quantum Electron. **QE-18**, 1062–1072 (1982).
4. D. Marcuse, "Single-channel operation in very long nonlinear fibers with optical amplifiers at zero dispersion," J. Lightwave Technol. **9**, 356–361 (1991).
5. R. Hui, D. Chowdhuri, M. Newhouse, M. O'Sullivan, and M. Poettcker, "Nonlinear amplification of noise in fibers with dispersion and its impact in optically amplified systems," IEEE Photon. Technol. Lett. **9**, 392–394 (1997).
6. A. Carena, V. Curri, R. Gaudino, P. Poggiolini, and S. Benedetto, "On the joint effects of fiber parametric gain and birefringence and their influence on ASE noise," J. Lightwave Technol. **16**, 1149–1157 (1998).
7. A. Mecozzi, "Long-distance transmission at zero dispersion: combined effect of the Kerr nonlinearity and the noise of the in-line amplifiers," J. Opt. Soc. Am. B **11**, 462–469 (1994).
8. A. N. Pilipetskii, E. A. Golovchenko, and S. G. Evangelides, Jr., "Nonlinear interaction of signal and noise in 10 Gb/s long distance RZ transmission," in *Optical Fiber Communication Conference*, 2000 OSA Technical Digest Series (Optical Society of America, Washington, D.C., 2000), paper FC4.
9. M. Midrio, F. Matera, and M. Settembre, "Reduction of amplified spontaneous emission noise impact on optically amplified systems in normal dispersion region of fibre," Electron. Lett. **33**, 1066–1068 (1997).
10. D. Marcuse, "Noise properties of four-wave mixing of signal and noise," Electron. Lett. **33**, 1175–1177 (1994).
11. J. M. Chávez Boggio, D. F. Grosz, A. Guimarães, and H. L. Fragnito, "Signal amplification by four-wave mixing in low-dispersion optical fibers," Microwave Opt. Technol. Lett. **23**, 318–320 (1999).
12. F. S. Yang, M. C. Ho, M. E. Marhic, and L. G. Kazovsky, "Demonstration of two-pump fibre optical parametric amplification," Electron. Lett. **33**, 1812–1813 (1997).
13. P. N. Butcher and D. Cotter, *The Elements of Nonlinear Optics* (Cambridge U. Press, Cambridge, 1991).
14. M. Yu, C. J. McKinstrie, and G. P. Agrawal, "Pump-wave effects on the propagation of noisy signals in nonlinear dispersive media," J. Opt. Soc. Am. B **12**, 1126–1132 (1995).
15. G. P. Agrawal, *Nonlinear Fiber Optics*, 2nd ed. (Academic, New York, 1995).
16. G. Cappellini and S. Trillo, "Third-order three-wave mixing in single-mode fibers: exact solutions and spatial instability effects," J. Opt. Soc. Am. B **8**, 824–838 (1991).
17. C. Mazzali, D. F. Grosz, and H. L. Fragnito, "Simple method for measuring dispersion and nonlinear coefficient near the zero-dispersion wavelength of optical fibers," IEEE Photon. Technol. Lett. **11**, 251–253 (1999).
18. M. Karlson, "Four-wave mixing in fibers with randomly varying zero-dispersion wavelength," J. Opt. Soc. Am. B **15**, 2269–2275 (1998).